Optimal Allocation and Sizing of Synchronous Condensers in Weak Grids with Increased Penetration of Wind and Solar Farms

Sajjad Hadavi, *Student Member, IEEE,* Milad Zarif Mansour, *Student Member, IEEE,* Behrooz Bahrani, *Senior Member, IEEE*

***Abstract*—The increasing number of weak-grid-connected renewable energy resources in power systems has created various challenges in recent years. Some examples include un-damped voltage oscillations in the ERCOT and sub-synchronous resonance in the North-China power grid. Several solutions for these challenges have been proposed, such as Static Compensators and Synchronous Condensers (SynCons). SynCons, being synchronous machines without a prime mover, provide several benefits in weak power systems, such as frequency support, system strength, and voltage regulation. Although SynCons are widely-utilized to mitigate the weak grid integration challenges, their installation/operation costs make them a costly solution. Additionally, their lead-time can be more than a year, which means their initial sizing and allocation must be optimal. In this paper, a method for the optimal allocation and sizing of SynCons is proposed. The main objective of this method is maintaining Short Circuit Ratio (SCR) in the system greater than pre-defined values while the investment and operation costs of SynCons, and voltage deviation in the system are minimized. Three meta-heuristic optimization algorithms are used to implement the proposed method, and its performance is evaluated via Electromagnetic Transient (EMT) time-domain simulation in a modified IEEE 39-bus system. The PSCAD/EMTDC software is used for the time-domain simulation. The simulation results confirm that with optimized allocation and sizing, the SCR of the network in all areas is more than pre-defined values, and also, all renewable energy resources can ride through disturbances and comply with given grid codes.**

***Index Terms*—Grid-Connected VSCs, Optimal Allocation, SCR, Solar Farm, Synchronous Condenser, Weak Grid, Wind Farm.**

I. Introduction

MAJORITY of renewable energy resources (RESs) are connected to power grids via power electronic converters (PECs) [1–4]. With an increasing number of PEC-connected generators, points in a power system that are distant from synchronous generators and close to PEC-connected ones experience low fault currents and low system strength. The prevalent index to quantify the weakness/strength of a power system is Short Circuit Ratio (SCR). Grids with SCRs of greater than three are categorized as strong ones, while SCRs below two indicate a very weak network [5].

Since many optimal sites for wind and solar farms have been already utilized, future developments need to focus on less desirable remote locations with low SCRs [6]. Additionally, points with rather high SCRs will experience lower SCRs as more PEC-connected generators are installed in their proximity. This results in a number of issues for wind/solar farms including but not limited to post-fault instability, failure to feed in full power stably under steady-state conditions, startup and re-synchronisation issues, control interactions and instability, cycling between turbine control modes, failure to ride-through disturbances, electromechanical oscillatory stability, and islanding issues [6–10].

To overcome these shortcomings, one approach is strengthening the grid by installing various compensators or reinforcing the grid infrastructure. Some examples of these solutions include transmission line reinforcement, battery energy storage technologies, synchronous condensers (SynCons), and static compensators (STATCOMs). Transmission lines are very costly and are not favorably seen by developers and network owners, and STATCOMs can only provide reactive power. Among these solutions, however, SynCons have regained popularity in recent years as they can provide voltage control, inject reactive power, and provide inertia to the system, simultaneously [11], [12]. SynCons are synchronous machines without a prime mover that do not generate electricity and only spin freely. Via regulating its field voltage, a SynCon is capable of regulating its reactive power exchange with the grid leading to strengthening the network to which it is connected [12]. Being a costly solution, SynCons capital cost can be justified if their rating and location are optimally selected [13], [14].

There are a limited number of studies on the optimal operation of SynCons and their impacts in weak grids [13], [15–18]. For example, in [15], a method to find the optimal location based on increasing impacts of SynCons in a power system and voltage stability is introduced. However, the SynCon installation cost and the effect of wind/solar farms penetration are not considered in this method. In [16], the post-retirement planning of existing synchronous machines is proposed to enhance the SCR and frequency response in a power system. The SynCons' location and size are based on the retired synchronous machines' capacity and location. If a retired synchronous machine's location is far from a new PEC-connected generator or the size of the retired synchronous machine is lower than a required value, it does not have sufficient impacts on the stability of the system. In [17], a method for optimal reactive power compensation using SynCons is proposed based on dynamic optimization. However, the proposed process is complex and time-consuming. Thus, it is not appropriate for a large system. Additionally, the effect of SynCons on the system's SCR is not investigated. In [18], an optimization procedure is employed to find the optimal location of SynCons based on increasing SCR and costs reduction in the system. However, the optimization of size and number of SynCons is neglected. Furthermore, there are not any tests to check compliance with standards and grid codes. Besides, none of the aforementioned studies considers the impacts of the installed PEC-generators on the SCR calculation.

In this paper, an optimization method to determine an optimal

number, allocation, and sizing of SynCons is introduced to enhance the system strength and stability in a large weak power system in the presence of wind and solar farms. The proposed method minimizes investment, operation, and maintenance costs of SynCons, and also voltage deviation in a system while the system's SCR is maximized at different nodes. Two different approaches are taken into account for the SCR calculation to ensure that the system strength is maximized. Since the SCR calculation based on SynCon allocation and sizing is a nonlinear problem, linear programming optimization approaches such as convex optimization are not applicable. Therefore, in this paper, three meta-heuristic optimization algorithms are adopted to implement the proposed optimization method with the lowest complexity and without any linearization. As the proposed method is simple and not time-consuming, it can be used for the system planning stage. The results are verified with Electromagnetic Transient (EMT) simulation in PSCAD/EMTDC software. The Australian grid code [19–21] is considered as a reference to examine the interaction of SynCons with wind and solar farms in a weak grid. Moreover, the optimized allocation/sizing of SynCons is compared with a random allocation/sizing. The main contribution of this paper as follows:

1) a comprehensive optimization method to minimize the SynCons overall cost and the system's voltage deviation at different buses,
2) consideration of grid codes standards in the optimization method,
3) consideration of PEC-connected generators and SynCons in the SCR calculation,
4) maintaining system strength in a large power system above a minimum requirement with minimum contribution of SynCons,
5) applying three different meta-heuristic algorithms for optimization.

The rest of the paper is organized as follows. The optimization method is introduced in Section II. In Section III, the proposed method is applied to an augmented IEEE 39-bus power systems to optimally allocate and size SynCons. In Section IV, the optimal values for allocation and sizing of SynCons are examined in an EMT simulation to validate the findings of Section III. Finally, Section V presents the conclusions of the paper.

II. Optimal Allocation and Sizing of SynCons

The principal objective of the proposed method is to reduce SynCons' investment, operating, and maintenance costs while the SCR of the system is increased. First, a mathematical model for the objective function is introduced. Then, the constraints of the objective function are determined. Finally, three heuristic optimization algorithms are chosen to implement the proposed method.

A. Objective Function

The principal objective function for the optimization method is defined as

$$F(x) = f_1(x) + f_2(x), \tag{1}$$

where $f_1(x)$ is the total investment, operation, and maintenance cost of SynCons, and $f_2(x)$ is the system's voltage deviation function. Since $f_1(x)$ and $f_2(x)$ have different scales, it is necessary to use a per-unit value for $f_1(x)$ and $f_2(x)$ in order to add them together in the objective function. The optimization algorithm minimizes $F(x)$ to minimize the total cost and voltage deviation. x is the input variable for the optimization algorithm, which consists of the number of SynCons, the locations of installation, and their sizes. This input is defined as

$$x = [N, \overline{X}_1, \overline{X}_2], \tag{2}$$

where N is the number of SynCons, $\overline{X}_1$ is a matrix of installation locations, and $\overline{X}_2$ is a matrix of SynCons' sizes. The dimension of $\overline{X}_1$ and $\overline{X}_2$ is equal to N. These inputs are formulated as

$$\begin{cases} \overline{X}_1 = [\mathrm{p}_1, ..., \mathrm{p}_i, ..., \mathrm{p}_N]_{1\times N} & 1 \le \mathrm{p}_i \le M \\ \overline{X}_2 = [\mathrm{s}_1, ..., \mathrm{s}_i, ..., \mathrm{s}_N]_{1\times N} & S_{\mathrm{SCmin}} \le \mathrm{s}_i \le S_{\mathrm{SCmax}} \end{cases}, \tag{3}$$

where M is the number of system's buses, S_{SCmin} is the minimum capacity of available SynCons, S_{SCmax} is the maximum capacity of available SynCons, and s_i and p_i are size and location of the i^{th} SynCon, respectively.

1) Total Cost: Being a very costly solution, to make it more attractive, SynCon's overall cost needs to be minimized. Assuming a power system with N SynCons, the overall SynCons' cost can be defined as

$$f_1(x) = \sum_{n=1}^{N} (\mathrm{C}_{\mathrm{i},n} + \mathrm{C}_{\mathrm{m},n} + \mathrm{C}_{\mathrm{o},n}) \frac{S_{\mathrm{SC}}}{S_{\mathrm{b}}}, \tag{4}$$

where $\mathrm{C}_{\mathrm{i},n}$, $\mathrm{C}_{\mathrm{m},n}$, and $\mathrm{C}_{\mathrm{o},n}$ are the n^{th} SynCon's investment cost, maintenance cost, and operational cost, respectively, based on their nominal capacity [14], [22]. S_{SC} and S_{b} are the capacity of the SynCon and the base MVA value of the power system, respectively.

2) Voltage Deviation: SynCons can change the load flow in the system, as they inject or absorb reactive power in the system. Thus, they can change the system's voltage. The minimization of steady-state voltage deviation, which is obtained by load flow, must be considered as the second objective function. This function can incorporate the grid codes margins in the optimization process. To fulfill this purposes, the Newton-Raphson algorithm is used to carry out the load flow analysis. Then, the voltage deviation for each bus can be defined as

$$\mathrm{VD}_b = \begin{cases} 0, & \text{if} \quad V_{\min} \le V_b \le V_{\max} \\ V_{\min} - V_b, & \text{if} \quad V_b \le V_{\min} \\ V_b - V_{\max}, & \text{if} \quad V_b \ge V_{\max} \end{cases}, \tag{5}$$

where VD_b is the voltage deviation for the b^{th} bus, $V_{\min}$ is the minimum acceptable value for the voltage in a system, and $V_{\max}$ is the maximum acceptable value for the voltage in a system. Then, $f_2(x)$ can be defined as

$$f_2(x) = \sum_{b=1}^{M} \mathrm{VD}_b, \tag{6}$$

where M is the number of system's buses.

In order to add flexibility to the objective function and ability to control the impact of each sub-objective function, weighting factors are added to the main objective function as

$$F(x) = w_1 f_1(x) + w_2 f_2(x), \tag{7}$$

where w_1 and w_2 are weighting coefficients for $f_1(x)$ and $f_2(x)$, respectively. Installing more SynCons increases system strength,

which can control voltage in the system due to contingencies. An increase in the system strength decreases voltage deviation from the desired values, however, it will result in higher cost. Similarly, reducing the size and number of SynCons reduces the cost, however, it can deteriorate the voltage deviation objective function. Therefore, the system operator must carefully choose w_1 and w_2. If the cost of SynCons is a more challenging aspect of their operation than the voltage deviation, w_1 must be larger than w_2. Otherwise, w_2 must be larger than w_1. Note that the summation of w_1 and w_2 must be equal to one, i.e., w_1+w_2=1. In this study, w_1=0.8, and w_2=0.2.

B. Constraints

SynCons are primarily utilized to strengthen the system. Thus, the system strength must be formulated in the optimization method. The common index to evaluate the weakness of a system is SCR. Therefore, the minimum SCR in a system is considered as an optimization constraint. The minimum SCR must be greater than a given value for all wind and solar farms point of connections (PoCs). In this paper, to guarantee a given system strength, two approaches are used for SCR calculation. The minimum value of the two approaches is considered as the SCR for the h^{th} PoC in the optimization method as

$$\mathrm{SCR}_h = \min(\mathrm{SCR}_{\mathrm{c},h}, \mathrm{SCR}_{\mathrm{m},h}),\ h = 1, .., k, \tag{8}$$

where k is the number of PoCs, and $\mathrm{SCR_c}$ and $\mathrm{SCR_m}$ are two approches to calculate SCR in a power system, which are described as follows.

1) $\mathrm{SCR_c}$*:* The common index to evaluate the weakness or strength of a power system is based on an equivalent impedance from the PoCs point of view. $\mathrm{SCR_c}$ for each PoC is defined as

$$\mathrm{SCR_c} = \frac{1}{Z_{\mathrm{eq}}}, \tag{9}$$

where Z_{eq} is the equivalent impedance of the system from a PoC point of view, in a per-unit system with a power base value equal to wind or solar farms generation capacity. Z_{eq} is obtained via the admittance matrix of a system. The admittance matrix, which is called Y_{bus} in power systems, has a dimension of M, which is the number of system's busses. The elements in Y_{bus} are

$$Y_{i,j} = \begin{cases} y_i + \sum_{n\neq i,\ n=1}^{M} y_{i,n} & ,\text{if } i = j \\ -\, y_{ij} & ,\text{if } i \neq j \end{cases}, \tag{10}$$

where $Y_{i,j}$ is the i,j^{th} element of Y_{bus}, y_i is self-admittance at the i^{th} bus, and y_{ij} is the admittance of the line between the i^{th} and the j^{th} buses. Additionally, the impedance matrix for a system, which is called Z_{bus}, is the inverse of Y_{bus} and is defined as

$$Z_{\mathrm{bus}} = Y_{\mathrm{bus}}^{-1}. \tag{11}$$

Since the diagonal element's value of the impedance matrix is the equivalent impedance for each bus, Z_{eq} for each PoC is defined as

$$Z_{\mathrm{eq}} = Z_{\mathrm{bus},ii}, \tag{12}$$

where $Z_{\mathrm{bus},ii}$ is the diagonal element's value of the impedance matrix for the i^{th} bus. The influence of loads in the system must be considered in the equivalent Z_{eq} assessment. To fulfill this purpose, all loads are modeled as R and X. The values for R and X can be obtained by their nominal active and reactive power consumption. In each optimization iteration, the Y_{bus} matrix is updated, and the impedance matrix is calculated. To update the admittance matrix, based on the location and size of SynCons, the diagonal element's value of the admittance matrix for the connection point is refreshed. A SynCon can be modeled as a current source and a parallel impedance. Fig. 1 depicts the SynCon model and the equivalent admittance of the system from the connection point. The new diagonal value in the admittance matrix is defined as

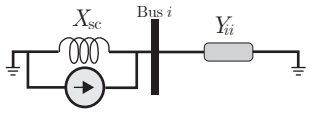

Fig. 1. The SynCon impedance model.

$$Y_{ii}^{\mathrm{new}} = Y_{ii}^{\mathrm{old}} + \frac{1}{jX_{\mathrm{sc}}}, \tag{13}$$

where X_{sc} is the SynCon's reactance. Therefore, the value of Z_{eq} changes with installation of SynCons.

2) $\mathrm{SCR_m}$*:* The main drawback of (9) is neglecting other VSCs effects in the system during a fault. VSCs can contribute to the fault current. Thus, the fault current must be calculated statically based on the proposed methods in [23]. The second SCR calculation method for each PoC, which considers the effects of VSCs in the fault current, is defined as

$$\mathrm{SCR_m} = \frac{V^{+}(0) \times I_{\mathrm{f}}}{P_{\mathrm{w,s}}}, \tag{14}$$

where $P_{\mathrm{w,s}}$ is the power generation of wind and solar farms is connected at PoC, $V^{+}(0)$ is the PoC voltage before the fault, and I_{f} is the fault current when a three-phase fault occurs at the PoC. To calculate I_{f} in a system, the injected current of other VSCs in a system and the SynCons injected currents are updated in each iteration of the optimization. Then, I_{f} is calculated based on the short circuit study proposed in [23].

To guarantee the SCR for each PoC is greater than a specific value, the SCRs must satisfy the following inequality

$$\mathrm{SCR}_h \geq R_h,\ h = 1, .., k, \tag{15}$$

where k is the number of PoCs, and R is a matrix that includes the minimum requirement for the PoCs' SCR. The boundary value for R_h is three.

C. Optimization Algorithms

To apply the proposed method, it is necessary to use an optimization algorithm. The SCR calculations, in particular, the second approach is a nonlinear problem. Furthermore, the voltage deviation calculation depends on the Newton-Raphson algorithm, which is a nonlinear procedure. Convex optimization methods cannot be used without any linearization and approximation for the proposed optimization method. Thus, meta-heuristic algorithms are utilized in this paper [24], [25].

The optimization procedure is summarized as Algorithm 1. As meta-heuristic optimization algorithms do not have unique solutions, it is necessary to use different kinds of algorithms to

avoid any local optimum solutions. In this paper, three meta-heuristic optimization algorithms are chosen. The solutions are compared to each other, and a set of solutions with the minimum objective function value or with the highest SCR at PoCs is chosen for the location and sizing of SynCons. These three algorithms are 1) Genetic algorithm (GA), 2) Bat algorithm, and 3) Hyper Spherical Search (HSS).

1) Genetic Algorithm: GA is one of the general meta-heuristic optimization algorithms used in power system studies [26], [27]. There is a biological science theory behind its concept. In this algorithm, based on stochastic computation, there is a set of possible solutions in each iteration for an optimization problem. These sets of solutions are called population. In each iteration, a set of the best solutions based on a fitness function is selected. In the next iteration, the GA creates the next set of solutions, a subset of the solutions in the previous iteration by crossover and mutation methods. The first population is selected randomly in the range of acceptable boundaries to achieve a global solution for the problem. This technique is useful for a wide range of applications, prevents local minimum answers if it is tuned properly, and can be beneficial for multi-objective problems. Also, it can solve problems with a large number of inputs [24].

2) Bat Algorithm: The Bat algorithm is inspired by the Bats navigation system. Bats adjust their direction and speed with a sonar technique to hunt foods or for navigation purposes. They spread a sound with a large and small amplitude and a specific frequency. Then, they receive its echo and analyze it to find where obstacle or food is. The Bat algorithm creates a set of solutions with specific characteristics randomly in the first iteration, with different specifications and then searches for the optimal solution among the solutions based on the Bats searching method. Then, the next iteration selects the solutions near the optimal solution and adjust new solutions by random flight, which includes a change in amplitude, frequency, and speed of previous iteration solutions. It can guarantee an optimal solution can be found [25]. The benefits of this technique are: 1) being easy to apply, 2) having a few parameters to tune, and 3) robustness.

3) Hyper Spherical Search: HSS has a space search mechanism, which is based on particles. HSS is similar to other meta-heuristic algorithms, and consist of some particles as individual possible solutions. The particles (solutions) converge to an optimum solution based on the objective function [28]. This algorithm specifies some features to particles such as radius and angle, which are related to the location of particles. In the HSS algorithm, population size and Hyper-sphere center particles must be defined. In the first iteration, a random set of individual particles (possible solutions) is defined based on the size of the population. Then, the best solutions are ranked, and the hyper-sphere center number of them are selected. In the next iteration, by changing the radius and angle of other particles, non-hyper-sphere center particles are moved to the hyper-sphere center space. The HSS procedure is stopped when all of the particles have the same value as the hyper-sphere center (optimum solutions). This algorithm is faster than other particle swarm optimization methods, and it is used in various power system problems such as optimal energy resources dispatch [28].

Algorithm 1 Optimization Procedure

Input: The power system information and minimum requirements for SCR

Output: The optimal number, location and capacity of SynCons

Start optimization algorithm (GA, Bat, or HSS):
Start a^{th} iteration:
Update x values based on the selected optimization algorithm
for $h = 1 : k$ **do**
Calculate Z_{eq} and I_{f}
Calculate SCR_{c} and SCR_{m}
end for
if $((\text{SCR}_{\text{c},h}$ & $\text{SCR}_{\text{m},h}) \geq R_h)$ **then**
Calculate $F(x)$
if $F(x)$ satisfies fitness function in optimization algorithm **then**
return $F(x)$ and x
else
go to iteration $a + 1$
end if
else
go to iteration $a + 1$
end if

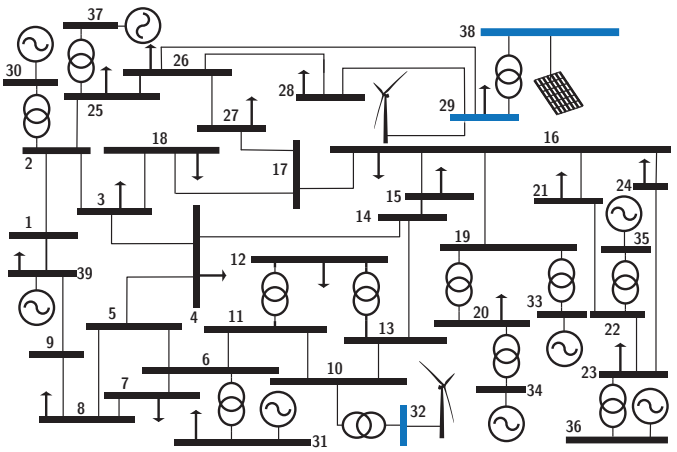

Fig. 2. Augmented IEEE 39-bus system.

III. Case Study and Optimization Results

In this section, the proposed method is implemented in a standard power system. The IEEE 39-bus system is chosen for the study [29]. This system is very stiff and does not have any renewable generation. Thus, some modifications such as increasing line's impedance and connection of wind or solar farms with long transmission lines are required to convert the system into a weak grid. Two wind farms and one solar farm are added to this weak grid. The nominal power of the installed RES are 200, 500, and 200 MW which are installed at Bus 29,32, and 38, respectively. Fig. 2 depicts the system's configuration. According to the mentioned modifications, the SCRs for PoCs are 2.6, 2.7, and 1.5 for Bus 29, 32, and 38, respectively.

The GA, HSS, and Bat algorithm are chosen to implement the proposed method. In this case, it is assumed at least three SynCons should be installed in the system. The maximum size of these SynCons is assumed to be 180 MVA. Table I

TABLE I
OPTIMIZATION RESULT FOR THE AUGMENTED IEEE 39-BUS

Optimization Method	Bus Number	Size	$F(x)$	SCR
GA	29, 29, 38, 38	13, 10, 118, 43	2.04	3.09
Bat	1, 38	11, 177	4	3
HSS	38, 38, 38	46, 10, 130	2.1	3.03

summarizes the optimization results for location and sizing of the SynCons with three optimization algorithms. The minimum SCRs in the system after applying the proposed method with three optimization algorithms are 3.09, 3, and 3.03 for the GA, Bat, and HSS algorithm, respectively. The minimum SCR with the GA optimization algorithm is higher than the other two techniques. Therefore, the solutions from the GA optimization is selected for further EMT simulation of this power system.

IV. PERFORMANCE EVALUATION WITH EMT SIMULATION

The purpose of this section is to verify the effectiveness of the optimized allocation and sizing of SynCons in the presence of wind and solar farms in the modified IEEE 39-bus system. To fulfill this purpose, PSCAD/EMTDC is selected for time-domain simulation of the modified IEEE 39-bus system. The components of the IEEE 39-bus system are modeled in detail in PSCAD/EMTDC. The generic model for a Type IV wind turbine and a solar farm are selected. Additionally, since exciters play a vital role in SynCons operation, it is critical to model the exciter in detail. In this paper, the AC1A model is selected for SynCons exciter modeling [30].

To evaluate the performance of the proposed method and analyze the transient stability of the system, the Australian National Electricity Rules (NER) are chosen as a benchmark [19]. According to the NER, wind and solar farms must remain connected during and subsequent to any contingency event. Farms must not create any oscillation such as Sub-Synchronous Oscillation (SSO) in the system as they can cause Sub-Synchronous Resonance (SSR) with the mechanical part of the power system, such as the shaft of synchronous generators. For transient stability analysis, Fault Ride Through (FRT) capability test and Multiple Fault Ride Through (MFRT) test are chosen. Solar and wind farms FRT strategy is based on the NER. If the voltage at the PoC becomes less than a V_{tresh} (in this study 0.85 pu), the FRT control mode is activated. Then, the Power Plant Controller (PPC) is deactivated, and the inverter injects reactive power based on the grid code standard. In the Australian grid code, the inverter must inject 4% of the maximum continuous current for each 1% voltage drop from V_{tresh}. Finally, to test small-signal stability of the proposed optimal allocation and sizing of SynCons, a step change is applied to each solar and wind farm in the system.

Furthermore, to evaluate the optimization results performance, Mean Square Error (MSE) and standard deviation (stdev) are used. MSE is the error value between an expected value of a signal and its real value, which is defined as

$$\text{MSE} = \frac{1}{l}\sum_{t=1}^{l}\left(W_i - \hat{W}\right)^2, \tag{16}$$

where l is the length of sampled data from voltage and output power signals, W_i is the i^{th} element of a data set, and $\hat{W}$ is a steady state value of a signal. In this study, the data set is recorded up to 2 s after a contingency clearance. Also, the steady-state value ($\hat{W}$) is a pre-contingency value of a signal. Moreover, the stdev is a signal measurement, which shows the distribution of a data set. If the stdev has a low value, it means data set values are close to the mean value. The stdev is calculated as

$$\text{stdev} = \sqrt{\frac{\sum\left(W_i - \mu\right)^2}{l}}, \tag{17}$$

where μ is a data set mean value.

A. FRT Test

In this test, for a single disturbance, a three-phase fault is considered as an event. The three-phase fault is applied at all wind and solar farms PoCs. According to the NER [19–21], wind and solar farms are required to ride through such a fault. In the simulation, a three-phase fault is applied at t=9.7 s. Also, the maximum time that breakers are allowed to fail in operation is 430 ms. Thus, the clearance time for the fault is considered to be 430 ms. The FRT test evaluates the farms' behavior in three scenarios. These scenarios are 1) the modified IEEE 39-bus system without SynCon, 2) the modified IEEE 39-bus system with the optimal allocation and sizing of SynCons, and 3) the modified IEEE 39-bus system with non-optimal allocation and sizing of SynCons.

1) FRT Test without SynCon: In this test, the three-phase fault is applied at all of the PoCs without installation of SynCons in the system. Prior to the fault in the system, the system is stable, the voltages are in the acceptable range, and the wind and solar farms generate their nominal power. The wind and solar farms at Bus 29 and 38 generate 200 MW, and the wind farm at Bus 32 generates 500 MW. However, subsequent to the FRT test, SSOs emerge in the system as shown in the following scenarios. When integrating RESs into weak grids, the voltage at a PoC is sensitive to contingencies. Therefore, the farms's phased-locked loop (PLL) cannot track the voltage at the PoC accurately. Furthermore, if the active power controller and current controller parameters are not well tuned, it can cause sustained oscillation in the system. Also, in a large power system with different RESs implemented, the RES controllers can interact with each other or with other installed equipment in the system such as capacitor bank or series capacitor and cause oscillation in the system [31–35]. Also, there are examples that report oscillations in various power systems around the world, such as sub-synchronous resonance in Electric Reliability Council of Texas (ERCOT) and the North-China power grid [6–8].

FRT Test on Bus 29: Fig. 3(a) depicts the voltages of all PoCs prior and subsequent to the three-phase fault, which is applied at Bus 29. Prior to the fault, the voltages are stable. Nevertheless, subsequent to the clearances of the fault, 12 Hz oscillation emerges in the system. The amplitude of this oscillation on the voltages at Bus 29 is significant (around 0.5 pu). Fig. 3(b) shows the wind farm's active and reactive power at Bus 29. Prior to the disturbance, the wind farm injects its nominal power 200 MW (1 pu) and 10 MVar (0.05 pu). During the fault, it contributes to voltage regulation and provides reactive power. However, subsequent to the fault clearance, the output active and reactive

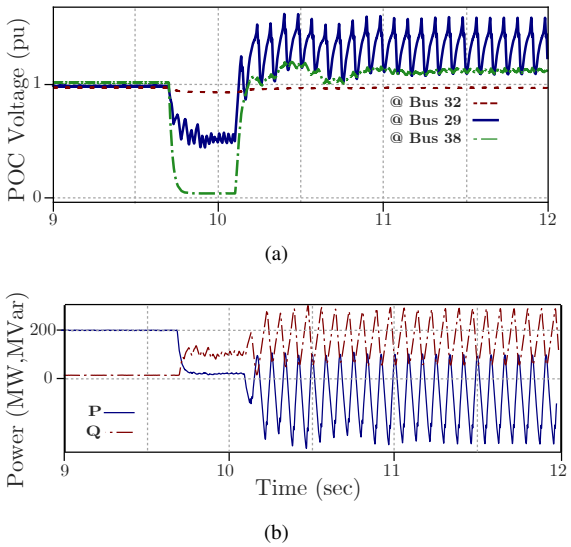

Fig. 3. Simulation results when the FRT test without SynCons is applied at t=9.7 s at Bus 29 with a duration of 430 ms: (a) bus voltages and (b) active and reactive power of the farm connected to Bus 29.

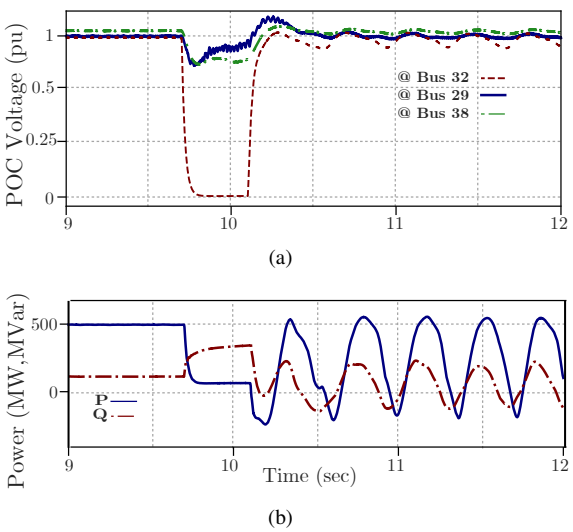

Fig. 4. Simulation results when the FRT test without SynCons is applied at t=9.7 s at Bus 32 with a duration of 430 ms: (a) bus voltages and (b) active and reactive power of the farm connected to Bus 32.

power cannot converge to their nominal values, and they oscillate with a frequency of 12 Hz. The magnitude of oscillations active power is more than 200 MW (1 pu) peak to peak. Thus, the wind farm at Bus 29 does not have FRT capability and makes the system unstable.

FRT Test on Bus 32: Without any contingency, the system is stable. The wind and solar farms are operated in their nominal condition, and the voltages are in an acceptable range. However, when the three-phase fault occurs at Bus 32, as it is shown in Fig. 4(a), 3 Hz SSO appears on the PoC voltages. The voltages at Bus 29 and 38 do not become zero during the fault. The reason is these buses are far from Bus 32. However, SSOs appear in Bus 29 and 38 voltages with a low amplitude. Additionally, based on Fig. 4(b), the wind farm's output active and reactive power are stable prior to and during the fault. The wind farm generates reactive power during the fault to recover the voltage, however, the active and reactive power cannot reach their nominal values subsequent to the fault clearance, and the system has 3 Hz sustained SSO. The amplitude of SSOs in active power is around 600 MW (1.2 pu), which is significant. Therefore, this wind farm does not have FRT capability.

FRT Test on Bus 38: Prior to the fault, the solar farm generates 200 MW, and the voltages in the system are stable. As shown in Fig. 5(a), Prior to the fault, all PoC voltages are stable and around 1 pu. During the fault, both Bus 29 and Bus 38 experience severe voltage dip because they are vicinity buses. Subsequent to the fault clearance, a 3 Hz SSO appears on the PoC voltages. For both Bus 29 and Bus 38, the amplitude of the oscillations is significant (0.2 pu peak to peak). Fig. 5(b) depicts the output power of the solar farm at Bus 38. During the fault, the solar farm contributes to voltage regulation by injecting reactive power. However, subsequent to the fault clearance, the output real and reactive power oscillate with a frequency of 3 Hz, whose amplitude is more than 200 MW (1 pu). Also, the solar farm at Bus 38 cannot provide its nominal power. In this case, The solar farm does not have FRT capability and causes instability in the system.

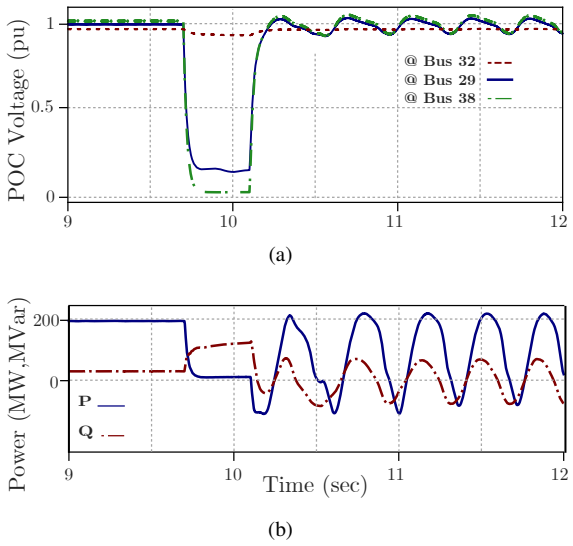

Fig. 5. Simulation results when the FRT test without SynCons is applied at t=9.7 s at Bus 38 with a duration of 430 ms: (a) bus voltages and (b) active and reactive power of the farm connected to Bus 38.

2) FRT Test with Optimized SynCons: This test is applied to all PoCs with the optimal allocation and sizing of SynCons based on the GA optimization algorithm results. Figs. 6(a), 6(b), and 6(c) show the PoC voltages when the fault is applied at Bus 29, 32, and 38, respectively. Additionally, Figs. 7(a), 7(b), and 7(c) show the farms output power when the fault is applied at Bus 29, 32, and 38, respectively.

FRT Test at Bus 29: As shown in Fig. 6(a), the voltages are stable prior to, during, and subsequent to the fault. All the PoC voltages have nominal values prior and subsequent to the fault. The PoC voltages reach an acceptable range subsequent to the fault clearance, and there is not any SSO in the system. The recovery time for the voltages, in this case, is 1.4 s subsequent to the fault clearance. Furthermore, Fig. 7(a) shows the wind farm active and reactive power, prior to, during, and subsequent to FRT test. As shown in Fig. 7(a), the active and reactive power are stable subsequent to fault clearance. Based on this test, it is

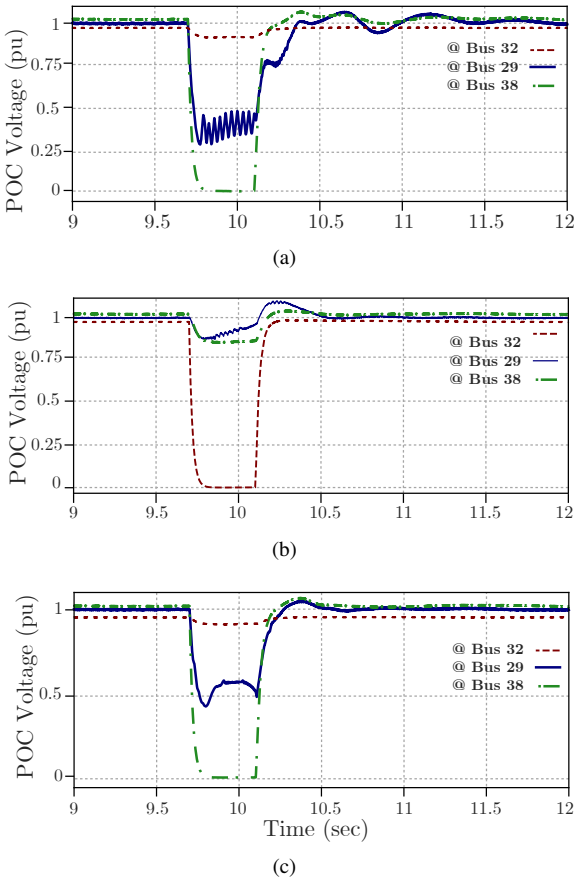

Fig. 6. Simulation results when the FRT test is applied at all PoCs at t=9.7 s with a duration of 430 ms with the optimal allocation and sizing of SynCons: (a) bus voltages when the FRT is applied at Bus 29, (b) bus voltages when the FRT is applied at Bus 32, and (c) bus voltages when the FRT is applied at Bus 38.

concluded the wind farm at Bus 29 has FRT capability.

FRT Test at Bus 32: Fig. 6(b) illustrates the PoC voltages. The system is stable after the FRT test. The voltages recover subsequent to the fault clearance in less than 0.5 s. The system is stable in this test and does not have SSO. Furthermore, Fig. 7(b) depicts the wind farm active and reactive power, prior to, during, and subsequent to FRT test. As depicted in Fig. 7(b), the active and reactive power are stable subsequent to the fault clearance, all of the oscillations are damped with the optimally sized and allocated SynCons. Also, the active and reactive powers do not have any oscillations during the fault and behave as it is expected from solar and wind farms. Thus, the wind farm at Bus 32 has FRT capability.

FRT Test at Bus 38: Fig. 6(c) shows the PoC voltages prior and subsequent to the FRT test at Bus 38. The voltages recover to their normal condition in 1 s subsequent to the fault clearance. Furthermore, Fig. 7(c) illustrates the solar farm active and reactive power, prior to, during, and subsequent to FRT test. As illustrated in Fig. 7(c), the active and reactive power are stable subsequent to fault clearance. The system is stable, and there are not any oscillations in the system. Thus, the solar farm at Bus 38 has FRT capability.

All of the wind and solar farms have the FRT capability with the optimal allocation and sizing of SynCons.

3) FRT Test with Random Allocation and Sizing of SynCons: To evaluate the optimized allocation and sizing of SynCons, it must be compared with a non-optimal allocation and sizing.

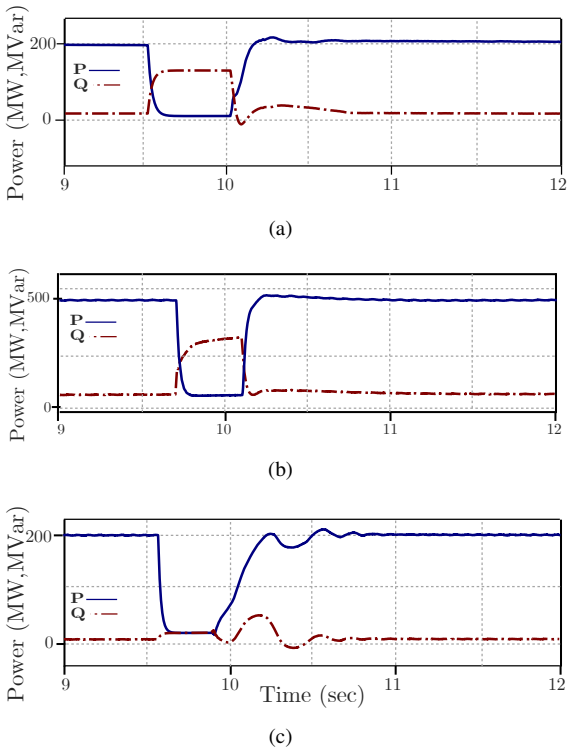

Fig. 7. Simulation results when the FRT test is applied at all PoCs at t=9.7 s with a duration of 430 ms with the optimal allocation and sizing of SynCons: (a) active and reactive power of the farm connected to Bus 29 when the FRT is applied at Bus 29, (b) active and reactive power of the farm connected to Bus 32 when the FRT is applied at Bus 32, and (c) active and reactive power of the farm connected to Bus 38 when the FRT is applied at Bus 38.

In this part, non-optimal allocation and sizing of SynCons is simulated. The FRT test is applied with a non-optimal utilization of SynCons in the modified IEEE 39-bus system. To fulfill the assessment, two scenarios are considered. In the first one, the SynCons are allocated in the system randomly with the optimal sizes. In the second one, the SynCons are allocated at the optimal positions based on the GA optimization algorithm's results. However, the SynCons' sizes are chosen randomly.

FRT Test with Random Allocation: In this test, the FRT test is applied at Bus 29 and 32 with the optimal number and size of SynCons, and non-optimal allocation of SynCons. The SynCons are located randomly at Bus 17 and 39 with optimal sizes. Fig. 8(a) depicts the PoC voltages prior to, during, and subsequent to the FRT test at Bus 29. Prior to the fault, the voltages are in the acceptable range, and the system is stable. Subsequent to the fault, 12 Hz SSO emerges in the system with a significant amplitude (around 0.5 pu peak to peak). Fig. 8(b) shows the PoC voltages subsequent to the FRT test at Bus 32 with random allocation of SynCons. As shown in Fig. 8(b), subsequent to the fault clearance, 3 Hz SSO appears in the system, which is not acceptable for the system operation. As shown in Fig. 8, the system is not stable after the non-optimally allocation of the SynCons. Thus, the non-optimal allocation of SynCons cannot help the wind and solar farms to gain FRT capability.

FRT Test with Random Sizing: In this test, the SynCons are allocated at the optimal locations based on Table I via the GA optimization results. However, their sizes are randomly selected. For one bus, larger than optimal values for the sizes of the

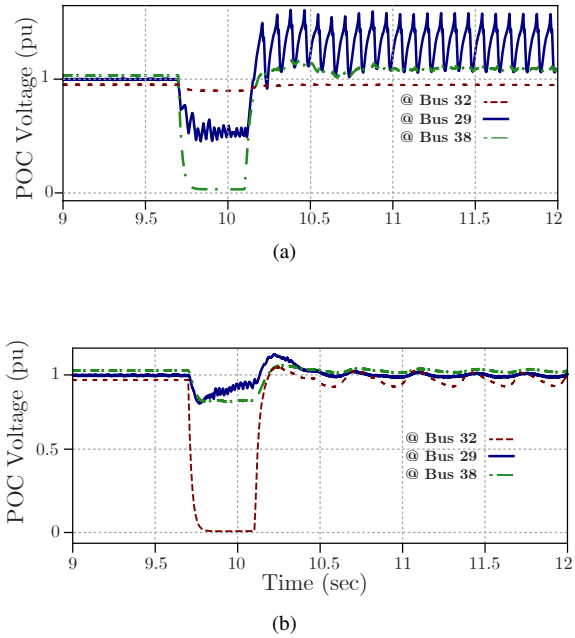

Fig. 8. Simulation results when FRT test is applied at two PoCs at t=9.7 s with a duration of 430 ms with random allocation of SynCons: (a) bus voltages when the FRT is applied at Bus 29 and (b) bus voltages when the FRT is applied at Bus 32.

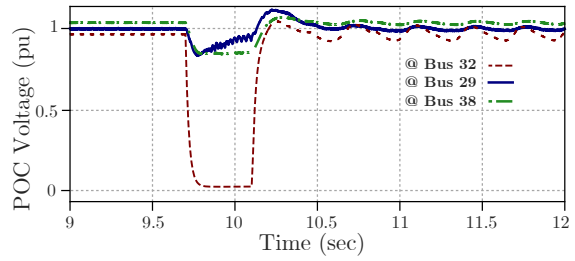

Fig. 9. Simulation results of bus voltages when FRT test is applied at Bus 32 at t = 9.7 s with a duration of 430 ms with random size of SynCons.

SynCons are selected, while for other optimal locations, lower than optimal values for the sizes of SynCons are selected. The SynCons' sizes at Bus 29 are 13 MVA and 20 MVA, and at Bus 38 are 80 MVA and 50 MVA. Therefore, the sizes of SynCons in the random sizing case at Bus 29 is larger than the optimal sizes and at Bus 38 lower than the optimal size. The FRT test is applied at the wind farm, which is connected at Bus 32. Fig. 9 illustrates the PoC voltages prior to, during, and subsequent to the FRT test at Bus 32. As shown in Fig. 9, subsequent to the FRT test at Bus 32, the system is not stable. There is SSO with a frequency of 3 Hz, which may cause SSR in the system. Therefore, the installation of the SynCons with the non-optimal sizes cannot help the wind and solar farms to have FRT capability even though larger than optimal SynCons are utilized at Bus 29. The main reason is the installation of smaller than optimal SynCons at Bus 38.

To analyse Fig. 3to Fig. 8, the MSE and stdev indices are calculated and listed in Table II. Table II shows a comparison of MSE and stdev indices of the PoC voltages in all scenarios and tests. The stdev and MSE are significantly lower in the optimized SynCons scenario compared to other scenarios in all tests. For instance, in the FRT test on Bus 32, the Bus 32 voltage's stdev value for the scenario with optimized SynCons is 0.005, which

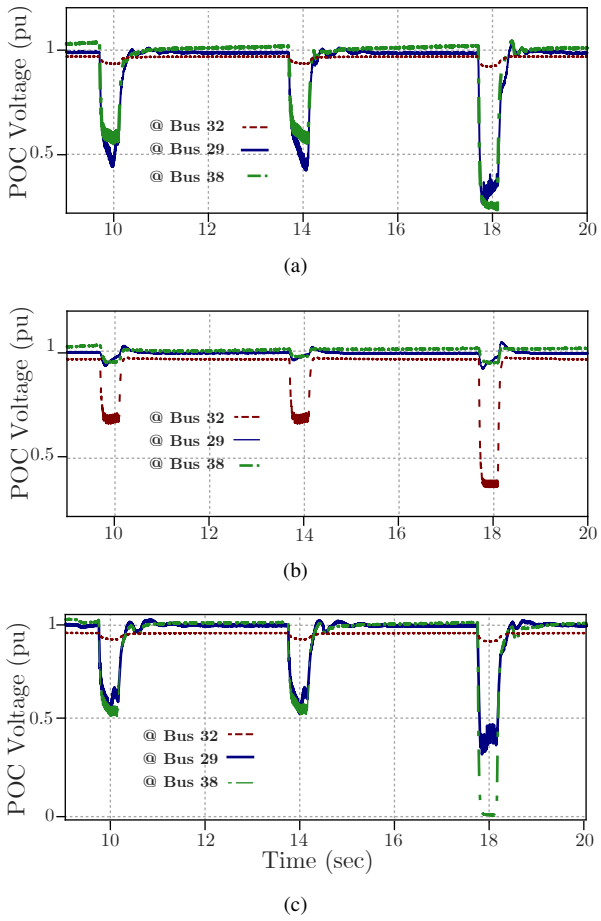

Fig. 10. Simulation results when the MFRT test is applied at the PoCs at t=9.7 s, t=13.7 s, and t=17.7 s with a duration of 430 ms by optimal allocation and sizing of SynCons: (a) bus voltages when the MFRT is applied at Bus 29, (b) bus voltages when MFRT is applied at Bus 32, and (c) bus voltages when the MFRT is applied at Bus 38.

is significantly lower than the other scenarios such as random sizing and random allocation.

B. MFRT Test with Optimized SynCons

According to the NER, wind and solar farms must ride through 15 disturbances in five minutes. The common disturbances for this test are three types of faults: 1) single-phase, 2) two-phase, and 3) three-phase faults. To assess the optimized optimal allocation and sizing of SynCons in a weak grid, the MFRT test is applied at the PoCs. The single-phase, two-phase, and three-phase faults are applied at t=9.7 s, t=13.7 s, and t=17.7 s, respectively. The duration of all three contingencies is 430 ms. The system must have MFRT capability and be stable subsequent to multiple faults. Fig. 10 illustrates the MFRT test at the PoCs. Fig. 10(a) to Fig. 10(c) illustrate the PoC voltages prior to, during, and subsequent to MFRT test, when it is applied at Bus 29, 32, and 38, respectively. As illustrated in Fig. 10, the system is stable subsequent to each fault, and the PoC voltages are in the acceptable range. The voltages come back to pre-fault conditions in less than 1 s subsequent to the fault clearance. Thus, the optimized allocation and sizing of the SynCons improves the system performance and add MFRT capability to the wind and solar farms.

TABLE II
POC VOLTAGES MSE AND STDEV VALUES FOR ALL TEST

Test	Signal	Scenario							
		without SynCons		with optimized SynCons		with random allocation		with random sizing	
		MSE	stdev	MSE	stdev	MSE	stdev	MSE	stdev
FRT test on Bus 29	Bus 29 Voltage	0.1349	0.1367	0.0044	0.06539	0.134	0.1353	-	-
	Bus 32 Voltage	0.000335	0.0143	1.4041e-05	0.00317	0.00034	0.0121	-	-
	Bus 38 Voltage	0.0188	0.05401	4.7774e-04	0.005143	0.017	0.0539	-	-
FRT test on Bus 32	Bus 29 Voltage	0.0011	0.0322	9.4220e-05	0.0097	0.001	0.0314	0.001	0.0314
	Bus 32 Voltage	0.0015	0.03269	3.1999e-05	0.005	0.00153	0.0357	0.00153	0.0327
	Bus 38 Voltage	0.001708	0.01298	4.9488e-05	0.0062	0.001	0.01	0.0023	0.014
FRT test on Bus 38	Bus 29 Voltage	0.00091774	0.0296	2.2594e-04	0.0069	-	-	-	-
	Bus 32 Voltage	2.0620e-05	0.00416	1.1182e-04	0.0025	-	-	-	-
	Bus 38 Voltage	0.0014	0.0349	2.1043e-04	0.00112	-	-	-	-

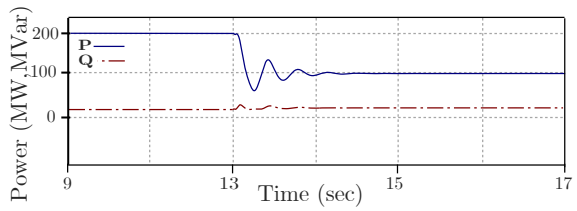

Fig. 11. Simulation results when a 50% active power step test is applied to wind farm at Bus 29 at t=13 s with the optimal allocation and sizing of SynCons.

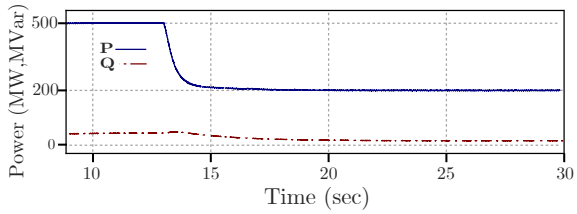

Fig. 12. Simulation results when a 60% active power step test is applied to wind farm at Bus 32 at t=13 s with the optimal allocation and sizing of SynCons.

C. Reference Power Step Test with Optimized SynCons

In this test, to evaluate the small signal stability of the system, a step change is applied to the reference active power of wind and solar farms connected to the system in the presence of optimally sized/allocated SynCons. The step is applied at t=13 s. According to the NER, wind and solar farms must respond to the active power step changes for a maximum of five minutes and operate stably after the change.

1) Active Power Step Test for the Wind Farm at Bus 29: As illustrated in Fig. 11, the wind farm injects 200 MW and 10 MVar prior to the step change. At t=13 s, the active power reference is changed to 100 MW, and the wind farm follows the new reference value and stably operate in the system.

2) Active Power Step Test at the Wind Farm at Bus 32: Fig. 12 shows the wind farm at Bus 32 injects 500 MW and 70 MVar prior to the step change in steady-state. At t=13 s, the active power reference is reduced to 200 MW, and the wind farm follows the new reference value and stably operate in the system.

3) Active Power Step Test for the Wind Farm at Bus 29: As depicted in Fig. 13, the wind farm injects 200 MW and 15 MVar prior to the step change. At t=13 s, the active power reference is changed to 100 MW, and the solar farm follows the new reference value and stably operate in the system.

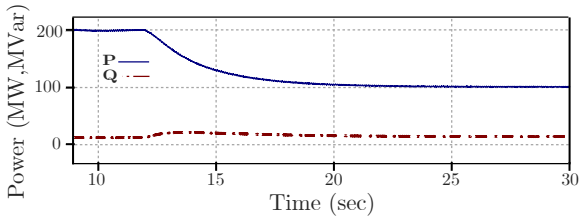

Fig. 13. Simulation results when an active power step test is applied to wind farm at Bus 38 at t=13 s with the optimal allocation and sizing of SynCons.

V. CONCLUSIONS

An optimization method for allocation and sizing of SynCons in weak power systems is proposed in this paper. The objective function of the proposed method is to maintain system strength greater than pre-defined values and minimizing SynCon installation/operation costs and voltage deviation in the system. The SCR index is used to assess the strength of the system. In the proposed method, the effects of the wind and solar farms, the system's loads, and SynCons on the SCR are considered. Furthermore, the optimization method is applied to a modified IEEE 39-bus test system via three Meta-heuristic optimization algorithms. The modified IEEE 39-bus test system is simulated in the PSCAD/EMTDC software to evaluate the performance of the proposed method and compliance of the system with the NER. The FRT and MFRT tests are applied to all of the PoCs. The simulation results demonstrate the effectiveness of the proposed method. The results show with the optimal allocation and sizing of SynCons, the wind and solar farms can earn FRT and MFRT capability.

REFERENCES

[1] X. Wang, L. Harnefors, and F. Blaabjerg, "Unified impedance model of grid-connected voltage-source converters," *IEEE Trans. Power Electron.*, vol. 33, no. 2, pp. 1775–1787, 2017.

[2] C. Phurailatpam, Z. H. Rather, B. Bahrani, and S. Doolla, "Measurement Based Estimation of Inertia in AC Microgrids," *IEEE Trans. Sustain. Energy.*, pp. 1–1, 2019.

[3] L. Fan, "Modeling type-4 wind in weak grids," *IEEE Trans. Sustain. Energy.*, vol. 10, no. 2, pp. 853–864, 2018.

[4] M. Nagpal and C. Henville, "Impact of power-electronic sources on transmission line ground fault protection," *IEEE Trans. Power Del.*, vol. 33, no. 1, pp. 62–70, 2017.

[5] J. Liu, W. Yao, J. Wen, J. Fang, L. Jiang, H. He, and S.-J. Cheng, "Impact of Power Grid Strength and PLL Parameters on Stability of Grid-Connected DFIG Wind Farm," *IEEE Trans. Sustain. Energy.*, 2019.

[6] "Connection of Wind Farms to Weak AC Networks," in *CIGRE Working Group Publication, WG B4.62.671*. CIGRE, 2016.

[7] H. Liu, X. Xie, C. Zhang, Y. Li, H. Liu, and Y. Hu, "Quantitative SSR analysis of series-compensated DFIG-based wind farms using aggregated RLC circuit model," *IEEE Trans. Power Syst.*, vol. 32, no. 1, pp. 474–483, 2016.

[8] H. Liu, X. Xie, J. He, T. Xu, Z. Yu, C. Wang, and C. Zhang, "Subsynchronous interaction between direct-drive PMSG based wind farms and weak AC networks," *IEEE Trans. Power Syst.*, vol. 32, no. 6, pp. 4708–4720, 2017.

[9] H. Liu, X. Xie, and W. Liu, "An Oscillatory Stability Criterion Based on the Unified *dq*-Frame Impedance Network Model for Power Systems With High-Penetration Renewables," *IEEE Trans. Power Syst.*, vol. 33, no. 3, pp. 3472–3485, 2018.

[10] R. Yang, G. Shi, X. Cai, C. Zhang, G. Li, and J. Liang, "Autonomous synchronizing and frequency response control of multi-terminal dc systems with wind farm integration," *IEEE Trans. Sustain. Energy.*, 2020.

[11] G. Zhou, D. Wang, A. Atallah, F. McElvain, R. Nath, J. Jontry, C. Bolton, H. Lin, and A. Haselbauer, "Synchronous Condenser Applications: Under Significant Resource Portfolio Changes," *IEEE Power and Energy Magazine*, vol. 17, no. 4, pp. 35–46, 2019.

[12] H. T. Nguyen, G. Yang, A. H. Nielsen, and P. H. Jensen, "Combination of synchronous condenser and synthetic inertia for frequency stability enhancement in low-inertia systems," *IEEE Trans. Sustain. Energy.*, vol. 10, no. 3, pp. 997–1005, 2018.

[13] F. O. Igbinovia, G. Fandi, Z. Müller, J. Švec, and J. Tlusty, "Cost implication and reactive power generating potential of the synchronous condenser," in *2016 2nd International Conference on Intelligent Green Building and Smart Grid (IGBSG)*. IEEE, Conference Proceedings.

[14] Y. Wang, F. Liu, H. Li, X. Wu, Y. Hou, and X. Zhao, "Synchronous Condenser Site Selecting Method for Reducing the Trip-off Risk of New Energy Generators," in *Proceedings of PURPLE MOUNTAIN FORUM 2019-International Forum on Smart Grid Protection and Control*. Springer, Conference Proceedings, pp. 75–83.

[15] F. O. Igbinovia, G. Fandi, Z. Müller, J. Švec, and J. Tlustý, "Optimal location of the synchronous condenser in electric-power system networks," in *2016 17th International Scientific Conference on Electric Power Engineering (EPE)*. IEEE, Conference Proceedings, pp. 1–6.

[16] N.-A. Masood, R. Yan, T. K. Saha, and S. Bartlett, "Post-retirement utilisation of synchronous generators to enhance security performances in a wind dominated power system," *IET Generation, Transmission & Distribution*, vol. 10, no. 13, pp. 3314–3321, 2016.

[17] Z. H. Rather, Z. Chen, P. Thøgersen, and P. Lund, "Dynamic reactive power compensation of large-scale wind integrated power system," *IEEE Trans. Power Syst.*, vol. 30, no. 5, pp. 2516–2526, 2014.

[18] J. Jia, G. Yang, A. H. Nielsen, E. Muljadi, P. Weinreich-Jensen, and V. Gevorgian, "Synchronous condenser allocation for improving system short circuit ratio," in *2018 5th International Conference on Electric Power and Energy Conversion Systems (EPECS)*. IEEE, Conference Proceedings.

[19] AMEC, "National Electricity Rules version 126," 2019.

[20] M. Mohseni and S. M. Islam, "Transient control of DFIG-based wind power plants in compliance with the Australian grid code," *IEEE Trans. Power Electron.*, vol. 27, no. 6, pp. 2813–2824, 2011.

[21] Y.-K. Wu, J.-H. Lin, and H.-J. Lin, "Standards and guidelines for grid-connected photovoltaic generation systems: A review and comparison," *IEEE Trans. Ind. Appl.*, vol. 53, no. 4, pp. 3205–3216, 2017.

[22] A. Tiwari and V. Ajjarapu, "Reactive Power Cost Allocation Based On Modified Power Flow Tracing Methodology," in *2007 IEEE Power Engineering Society General Meeting*, Conference Proceedings, pp. 1–7.

[23] J. Jia, "Assessment of Short Circuit Power and Protection Systems for Future Low Inertia Power Systems," Ph.D. dissertation, Technical University of Denmark, Department of Electrical Engineering, 2018.

[24] A. Askarzadeh, "A memory-based genetic algorithm for optimization of power generation in a microgrid," *IEEE Trans. Sustain. Energy.*, vol. 9, no. 3, pp. 1081–1089, 2017.

[25] K. S. Tey, S. Mekhilef, and M. Seyedmahmoudian, "Implementation of BAT Algorithm as Maximum Power Point Tracking Technique for Photovoltaic System Under Partial Shading Conditions," in *2018 IEEE Energy Conversion Congress and Exposition (ECCE)*. IEEE, Conference Proceedings, pp. 2531–2535.

[26] A. Keane, L. F. Ochoa, C. L. Borges, G. W. Ault, A. D. Alarcon-Rodriguez, R. A. Currie, F. Pilo, C. Dent, and G. P. Harrison, "State-of-the-art techniques and challenges ahead for distributed generation planning and optimization," *IEEE Trans. Power Syst.*, vol. 28, no. 2, pp. 1493–1502, 2012.

[27] A. H. Yazdavar, M. F. Shaaban, E. F. El-Saadany, M. Salama, and H. H. Zeineldin, "Optimal planning of distributed generators and shunt capacitors in isolated microgrids with nonlinear loads," *IEEE Trans. Sustain. Energy.*, 2020.

[28] H. Karami, M. J. Sanjari, and G. B. Gharehpetian, "Hyper-Spherical Search (HSS) algorithm: a novel meta-heuristic algorithm to optimize nonlinear functions," *Neural Computing and Applications*, vol. 25, no. 6, pp. 1455–1465, 2014.

[29] W. Sun, C.-C. Liu, and L. Zhang, "Optimal generator start-up strategy for bulk power system restoration," *IEEE Trans. Power Syst.*, vol. 26, no. 3, pp. 1357–1366, 2010.

[30] K. Máslo, A. Kasembe, and M. Kolcun, "Simplification and unification of IEEE standard models for excitation systems," *Electric Power Systems Research*, vol. 140, pp. 132–138, 2016.

[31] W. Du, Q. Fu, and H. Wang, "Subsynchronous oscillations caused by open-loop modal coupling between vsc-based hvdc line and power system," *IEEE Trans. Power Syst.*, vol. 33, no. 4, pp. 3664–3677, 2017.

[32] W. Du, Q. Fu, H. Wang, and Y. Wang, "Concept of modal repulsion for examining the subsynchronous oscillations caused by wind farms in power systems," *IEEE Trans. Power Syst.*, vol. 34, no. 1, pp. 518–526, 2018.

[33] H. Liu, X. Xie, J. He, T. Xu, Z. Yu, C. Wang, and C. Zhang, "Subsynchronous interaction between direct-drive pmsg based wind farms and weak ac networks," *IEEE Trans. Power Syst.*, vol. 32, no. 6, pp. 4708–4720, 2017.

[34] W. Ren and E. Larsen, "A refined frequency scan approach to subsynchronous control interaction (ssci) study of wind farms," *IEEE Trans. Power Syst.*, vol. 31, no. 5, pp. 3904–3912, 2015.

[35] G. Stamatiou and M. Bongiorno, "Stability analysis of two-terminal vsc-hvdc systems using the net-damping criterion," *IEEE Trans. Power Del.*, vol. 31, no. 4, pp. 1748–1756, 2016.

Sajjad Hadavi (S'19) received the B.Sc. and M.Sc. degrees in electrical engineering from Amirkabir University of Technology, Tehran, Iran, in 2013 and 2015, respectively. Since 2018 he has been pursuing a Ph.D. degree at Monash University, Australia. His research interests include control of power electronics systems, power electronics in power systems, and grid integration of renewable energy resources.

Milad Zarif Mansour received the B.Sc. degree from the University of Tehran, Tehran, Iran, and the M.Sc. degree from Sharif University of Technology, Tehran, Iran, both in electrical engineering, in 2016 and 2018, respectively. Since 2019, he has been with Monash University as a Ph.D. student. His research interests include grid integration of renewable energy resources, control of power electronic devices, and applications of power electronics in power systems.

Behrooz Bahrani Behrooz Bahrani (M'13–SM'19) received the B.Sc. degree from Sharif University of Technology, Tehran, Iran, the M.Sc. degree from the University of Toronto, Toronto, ON, Canada, and the PhD degree from the Ecole Polytechnique Fédérale de Lausanne (EPFL), Lausanne, Switzerland, all in electrical engineering, in 2006, 2008, and 2012, respectively. From September 2012 to September 2015, he was a Postdoctoral Fellow at several institutions including EPFL, Purdue University, West Lafayette, IN, USA, Georgia Institute of Technology, Atlanta, GA, USA, and the Technical University of Munich, Munich, Germany. Since 2015, he has been with Monash University, Clayton, Australia, where currently, he is a Senior Lecturer and the Director of the Grid Innovation Hub. His research interests include control of power electronics systems, applications of power electronics in power and traction systems, and grid integration of renewable energy resources.